Microelectronic Engineering 93 (2012) 39–42

Contents lists available at SciVerse ScienceDirect

Microelectronic Engineering

journal homepage: www.elsevier.com/locate/mee

Accelerated Publication

Carbon nanotube thin film pH electrode for potentiometric enzymatic acetylcholine biosensing

Dongjin Lee [1], Tianhong Cui *

Department of Mechanical Engineering, University of Minnesota, USA

ARTICLE INFO

Article history:
Received 17 December 2010
Received in revised form 8 October 2011
Accepted 29 October 2011
Available online 9 December 2011

Keywords:
Carbon nanotube
pH sensor
Thin film
Electrochemical biosensor
Acetylcholine sensor

ABSTRACT

Carboxylated single-walled carbon nanotube thin-film (SWCNT-TF) is demonstrated as a pH electrode and a platform for enzymatic potentiometric acetylcholine biosensors. SWCNT is layer-by-layer assembled with a positively charged polyelectrolyte on the metal electrode. The open circuit potential on SWCNT-TF electrode is measured with reference to an Ag/AgCl electrode in various pH buffers. With the aid of acetylcholinesterase (AchE), acetylcholine (Ach) is successfully detected using the SWCNT-TF pH electrode that demonstrates Nernst potential of −43 mV/pH. AchE-modified electrode has a sensing resolution of 10 μM of Ach and sensitivity of 19 mV/decade. The SWCNT-TF pH electrode fabricated by layer-by-layer self-assembly may play an important role in micro/nanoscale electrochemical sensors.

1. Introduction

Carbon nanotube (CNT) has been spotlighted for a variety of applications such as transistors [1,2], sensors [3,4], actuators [5], and solar cells [6] due to the excellent mechanical, electrical, thermal, and optical properties with a high degree of chemical and thermal stability. Particularly, the unique electrochemical properties of CNTs enable them to be utilized for chemical and biological sensing [7]. The interaction of CNTs with biological entities such as enzyme, DNA, and antibody could be enhanced due to the size similarity. In addition, an extremely small size is suitable to develop micro/nanoscale functional structures for broad spectrum of applications.

The ionic concentration plays a biologically important role. For example, mitogenic stimulation on cell division leads to ionic concentration changes, so that $[Ca^{2+}]$ and pH in cytoplasm are indications of progression to DAN synthesis after the fertilization [8]. Therefore, a miniaturized ion sensing probe is required to monitor and read out pH *in situ* with a high resolution. So far, electrochemical ion sensors have been implemented as the ion selective electrodes (ISE) that comprises solid electrode, internal filling solution, and ion-selective membrane, which makes it hard to maintain and miniaturize. The necessity of micro/nanoscale electrode along with facile maintenance leads to development of potentiometric solid-state electrodes such as coated wire electrode. However, solid contact between conducting electric wire and ion-selective membrane has poor mechanical adhesion and insufficient electrochemical stability [9], thereby resulting in irreproducible potential throughout lifetime [10].

The ion-sensitive field-effect transistor (ISFET), as a pH electrode, is based on the ion-sensitive or selective membrane that replaces the gate electrode in metal oxide field-effect transistors. The behavior of ISFET is completely controlled by the electrolyte/insulator interface by forming membrane potential, which plays the role of gate voltage in ISFET, thereby yielding different output signal depending on the specific ion concentration. ISFET sensors have been constructed in conjunction with exceptional nanomaterial properties [11,12]. Layer-by-layer assembled indium oxide (In_2O_3) nanoparticles (NPs) and single-walled carbon nanotubes (SWCNTs) had sensitive electric properties to pH. It turned out that nanomaterial based ISFETs had a higher sensitivity and resolution than the conventional silicon based ISFET presumably due to the unique properties and large surface-to-volume ratio. The randomly networked SWCNT based ISFET [13] was also reported to have detection limit of 10 nM of K^+.

The acetylcholine (Ach) is the neurotransmitter that activates the muscle and forms the cholinergic system with associated neurons causing excitatory action. Specifically, the malfunction of the cholinergic system in the brain causes Alzheimer's disease (AD) characterized by the memory deficits. Ach is the ester that is hydrolyzed via acetylcholinesterase (AchE) enzyme as follows:

* Corresponding author. Address: 111 Church St. S.E., Minneapolis, MN 55455, USA. Tel.: +1 612 626 1636; fax: +1 612 625 6069.
E-mail address: tcui@me.umn.edu (T. Cui).
[1] Current address: School of Mechanical Engineering, Konkuk University, 120 Neungdong-ro, Gwangjingu, Seoul 143-701, Republic of Korea.

0167-9317/$ - see front matter © 2011 Elsevier B.V. All rights reserved.
doi:10.1016/j.mee.2011.10.017

$$CH_3COO(CH_2)_2N^+(CH_3)_3 + H_2O \xrightarrow{AchE} CH_3COO^- + H^+ + HO(CH_2)_2N^+(CH_3)_3$$

Most Ach sensors reported used the amperometric [14–19] or potentiometric [20–22] electrochemical transduction mechanism. Particularly, novel nanomaterial ISFET sensors for Ach have been developed using self-assembled In_2O_3 NPs [21] and SWCNTs [22]. Layer-by-layer assembled nanomaterials were used as the semiconducting channel in conductometric sensors where charge carriers were enhanced or reduced depending on bulk solution [23]. The pH change in bulk solution was detected by the mutation of conductivity of nanomaterial thin-film. However, the existence of silica NPs on top of semiconducting layer precludes the estimation of sensing principles and development of novel types of sensors. The potential difference between bulk sample solution and nanomaterial thin-film was considered due to the abundant surface functional groups on SWCNTs by employing a simple structure. It also excludes the effect of silica NPs, so that the sensing performance of SWCNT itself will be evaluated. Meanwhile, carboxylated SWCNTs multilayer has played the role of polyacid [24], where protonation/deprotonation occurs on CNT thin-film, leading to changes in electrical conductance of thin-film. It is speculated that CNTs could be exploited as ion-selective electrodes (ISEs) and biosensors due to the abundant functional groups on nanotubes. Therefore, carboxylated SWCNTs were directly used as a pH electrode in this letter. The open circuit potential on the SWCNT thin-film (SWCNT-TF) was measured with reference to Ag/AgCl electrode to demonstrate the behavior of pH electrode. Furthermore, SWCNT-TF pH electrode was extended to detect the Ach potentiometrically with the aid of AchE that had been physically adsorbed on SWCNTs. Ach is hydrolyzed to carboxylic acid and choline, resulting in local pH shift in the vicinity of SWCNTs. The collection of protons in SWCNT-TF induced the change of electrode potential versus Ag/AgCl reference electrode in response to Ach concentration. The self-assembled SWCNT-TF could be used as solid-state pH electrode and serve as a platform for enzymatic biosensing.

2. Experimental

Chemical functionalization of SWCNTs was performed following previous works [24,25]. SWCNTs of 0.5 g (Nanostructured and Amorphous Materials, purity: 90% of SWCNTs and 95% of CNTs, diameter: 1–2 nm, length: 5–30 μm, SSA: 300–380 m^2/g) were chemically functionalized in 3:1 mixture of concentrated sulfuric (150 mL, H_2SO_4) and nitric acid (50 mL, HNO_3) at 110 °C for an hour. The mixture was diluted into water 5-fold and vacuum filtered with the pore size of 0.22 μm. After the rinsing with deionized water several times until pH approached 5.5, the functionalized SWCNTs (f-SWCNTs) were collected and re-dispersed into 500 mL of fresh deionized water under ultra-sonication for an hour. The SWCNT solution was centrifugated at a speed of 5000 rpm (4500*g*, Eppendorf centrifuge 5804) for 20 min. Finally, the supernatant was carefully decanted and the precipitates were discarded. The final concentration of SWCNT solution was about 0.6 mg/mL (0.06 wt.%). Fourier transform infrared spectrometer (FTIR, Nicolet Magna IR 750) was used to characterize the surface functional groups after the acidic treatment.

Polyelectrolytes used were poly(diallyldimethylammonium chloride, PDDA, M_w = 200–350 k, Aldrich) and poly(styrenesulfonate, PSS, M_w = 70 k, Aldrich). The concentration of PDDA and PSS aqueous solution used for LbL self-assembly was 1.4 and 0.3 wt.%, respectively, with 0.5 M sodium chloride (NaCl).

Starting with on silicon (Si) wafer with thermally grown silicon dioxide (SiO_2) 2 μm thick, chromium (Cr, 300 Å) and gold (Au, 1000 Å) were deposited with electron-beam evaporation system

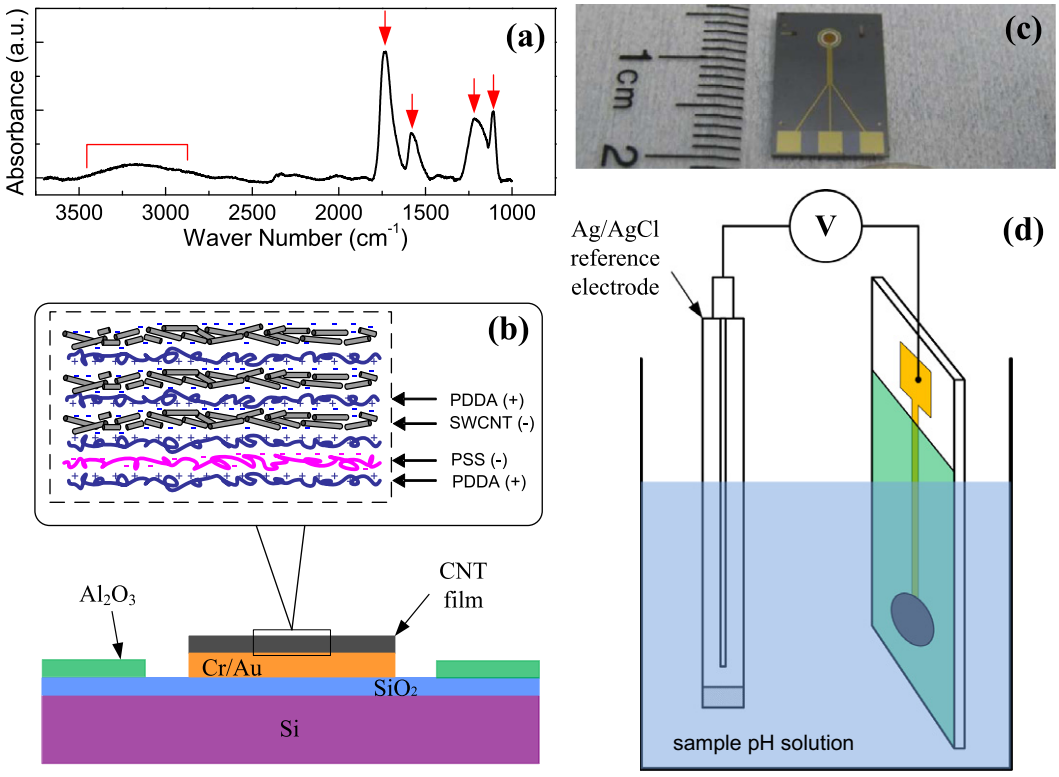

Fig. 1. Layer-by-layer assembled carboxylated carbon nanotube thin film pH electrode for biosensing: (a) FTIR spectrum of functionalized carbon nanotubes, (b) schematic of device section as a working electrode, (c) photo of fabricated device, and (d) testing apparatus.

(SEC 600, CHA Industries Inc.). Photolithographic patterning was done for the metal electrode which was circular shape with a diameter of 1 mm. Dielectric aluminum oxide (Al_2O_3) was deposited with atomic layer deposition (ALD) as a passivation layer to prevent unwanted electrochemical reaction on the elongated electrode. Another photolithography was performed to make opening window of photoresist for layer-by-layer (LbL) assembled SWCNTs. LbL assembly was done as previously reported [24] to produce a hierarchical structure of [PDDA (10 min)/PSS (10 min)]$_2$ + [PDDA (10 min)/SWCNT (15 min)]$_5$. Fabricated sensors were tested in various standard pH buffers that were formulated by Na_2HPO_4 and NaH_2PO_4 with buffering power of 80 mM. The open circuit potential was measured between Ag/AgCl reference electrode and SWCNT-TF working electrode. Additional enzymatic layer was formed by LbL assembly of {PDDA (10 min) + [PSS (10 min)/AchE (10 min)]$_3$} for the detection of Ach. Standard 10-fold serial dilutions of Ach aqueous solution was prepared using 1× phosphate buffered saline (PBS, pH 7.2, GIBCO).

3. Results and discussion

The absorption spectrum of f-SWCNT is shown in Fig. 1a. The characteristic peaks are shown at the wave numbers of 1730, 1580, 1150 and 1105 as well as the broadband of 3100–3500 cm^{-1}. Particularly, the sharp peaks at 1730 and 1150 cm^{-1} are originated from the stretching vibration of C=O and C–O, respectively, which are considered as the obvious indication of the functionalization of SWCNTs with carboxylic groups [26]. In addition, the broadband on the range of 3000–3500 cm^{-1} is caused by the stretching of –OH in the carboxylic acids [27]. The peak at 1580 cm^{-1} is ascribed to the intrinsic property of SWCNTs characterized by C=C stretching vibration [26]. The sharp peak observed at 1105 cm^{-1} might be attributed to Si–O–Si vibration of the Si/SiO_2 substrate used [27]. Therefore, it is obvious that carboxylic and/or hydroxyl groups are materialized as a result of the chemical treatment.

The device structure is schematized in Fig. 1b, where SWCNT multilayer was deposited on top of Cr/Au metal electrode. The area other than the electrode is covered with Al_2O_3 as a passivation layer. The photograph of an individual chip is shown in Fig. 1c. Each individual chip is in size of 1 by 1.5 cm^2. Sensing area of SWCNT pattern has the diameter of 1 mm. The open circuit potential measurement was performed on 24-well plate as shown in Fig. 1d with respect to the commercial miniaturized Ag/AgCl reference electrode (Cypress Systems, EE008) with internal filling solution of 3 M KCl. The distance between the reference electrode and sensing chip was kept constant at 5 mm.

LbL assembled SWCNTs were characterized by scanning electron microscope (Jeol 6700F) with the acceleration voltage of 5 kV, and the result is depicted in Fig. 2a, where individual SWCNTs, bundles, and random network of those are clearly observed. The Cr/Au metal electrode modified with SWCNT-TF and AchE uses two reaction mechanisms: enzymatic reaction followed by H^+/OH^- detection in solid-state SWCNT-TF as a pH electrode. Fig. 2a shows the schematic of operating principle of LbL assembled SWCNTs as a pH electrode. Hydrogen ions produced in enzymatic hydrolysis diffuse toward the bulk sample solution or into SWCNT-TF. Once the stable hydrogen ion distribution forms, the electrode potential versus Ag/AgCl reference electrode has been

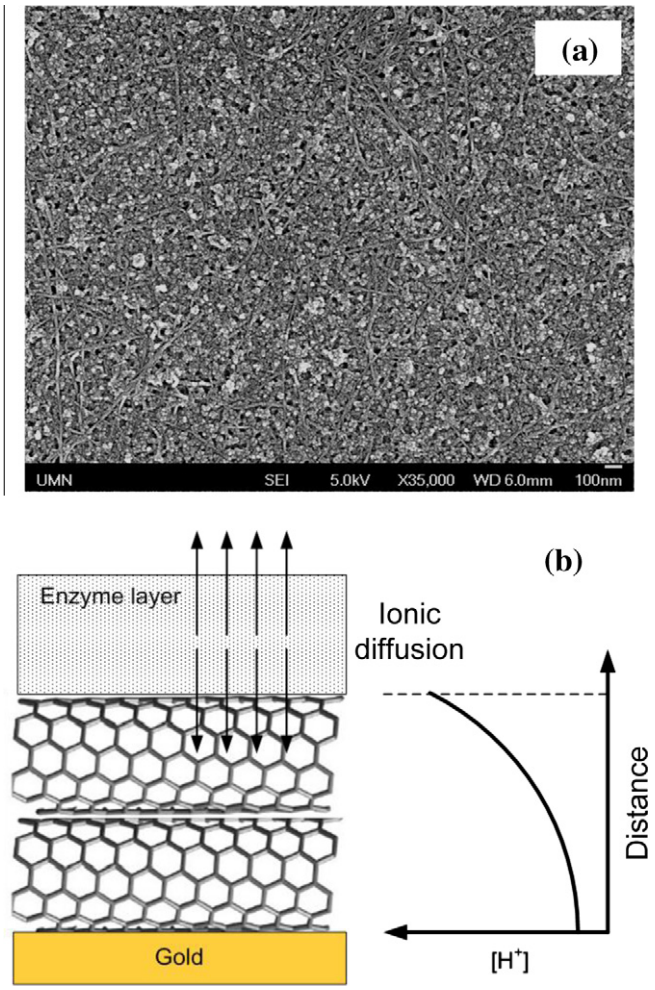

Fig. 2. Scanning electron microscope image of SWCNT thin film on top of metal electrode (a) and hydrogen ion distribution inside SWCNT thin film explaining the operating principle of electrode potential as a biosensor.

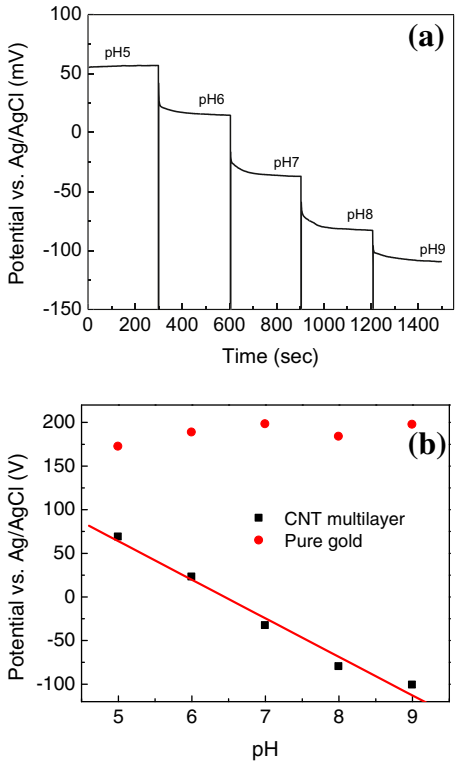

Fig. 3. pH sensing of SWCNT thin film: (a) time response of open circuit potential from pH 5 to 9 and (b) pH-responsive open circuit potentials at various pH buffers.

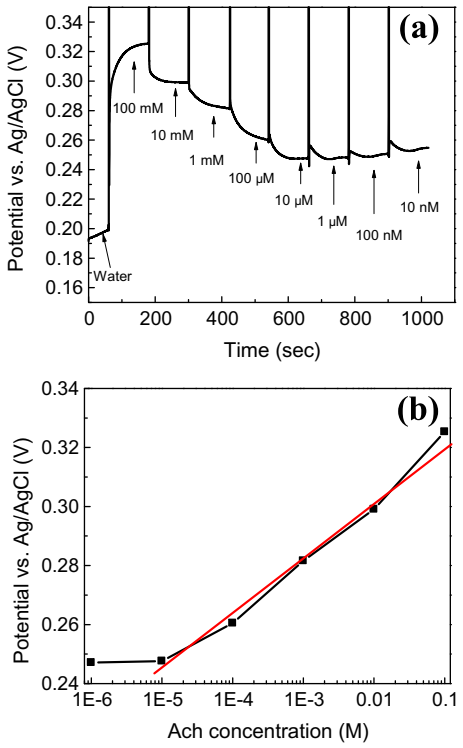

Fig. 4. Acetylcholine sensing of SWCNT thin film with AchE enzymatic layer: (a) time response of open circuit potential from 100 mM to 10 nM and (b) Ach-responsive open circuit potentials at various Ach concentrations.

determined. The electrode potential is dependent on pH at the enzyme layer due to the capability of capturing hydrogen ions on the large quantity of carboxylated SWCNTs [24].

H^+/OH^- detection mechanism was verified for biosensing application in various pH buffer solutions without AchE layer. The result of pH sensing is shown in Fig. 3. Time responses were measured from pH 5 to pH 9 buffer solution as shown in Fig. 3a. Once a stable signal was obtained, SWCNT-TF electrode and Ag/AgCl reference electrode were dipped into a different pH buffer without intermediate washing of the electrode surface. SWCNT-TF pH electrode showed a time constant of about 2 min. The stable open circuit potentials are shown as a function of pH in Fig. 3b with the control electrode without SWCNT-TF on the Cr/Au metal electrode. While slightly increasing voltage signal was observed on bare gold surface from 0.172 to 0.198 V, the linear relationship was found on the LbL assembled SWCNT-TF. As a result, the Nernstian response of −43 mV/pH was obtained ($R^2 = 0.9903$). This suggests that SWCNT-TF plays the role of solid-state pH electrode.

The enzyme layer of (PSS/AchE) enabled SWCNT pH electrode to be utilized as Ach sensors. AchE enzymes convert the Ach substrate solution to produce pH change, which was measured with the underlying SWCNT-TF. SWCNT-TF with AchE was characterized at various Ach concentrations as shown in Fig. 4. The electrodes were firstly immersed into deionized water and dipped into the serial 10-fold dilutions of Ach into PBS starting from 100 mM to 10 nM as depicted in Fig. 4a. The SWCNT-TF with AchE showed the response time of about 1 min. The stable potentials are replotted as a function of Ach concentration as shown in Fig. 4b. The sensor showed a resolution of 10 μM. Although it is lower than reported CNT film conductometric type [23], it might be enhanced through the tuning of electrochemical properties of CNTs. The sensitivity was found as 19 mV/decade ($R^2 = 0.9879$) on the range of 10 μM–100 mM. Other enzyme–substrate systems that produce pH shift could be detected using SWCNT-TF pH electrode.

4. Conclusion

The carboxylated SWCNT-TF demonstrates that the solid-state carbon nanotube pH electrode possesses linearly decreasing potential referenced to the Ag/AgCl reference electrode with the increasing pH values. With the aid of acetylcholinesterase enzymatic reaction accompanying pH change, acetylcholine was successfully detected potentiometrically down to 10 μM. The elaborate tuning of electrochemical properties of self-assembled SWCNTs can be expected through the chemistry of nanotube and versatility of layer-by-layer assembly. The solid-state SWCNT-TF pH electrode may play an important role in micro/nanoscale electrochemical sensors.

Acknowledgments

The authors gratefully acknowledge the support of NSF Grant No. CMMI 0735268. Parts of this work were carried out in the Characterization Facility and the Nanofabrication Center, University of Minnesota, which are partially supported by NSF.

References

[1] R. Martel, T. Schmidt, H.R. Shea, T. Hertel, P. Avouris, Appl. Phys. Lett. 73 (1998) 2447–2449.
[2] M.C. LeMieux, M. Roberts, S. Barman, Y.W. Jin, J.M. Kim, Z. Bao, Science 321 (2008) 101–104.
[3] E.S. Snow, F.K. Perkins, J.A. Robinson, Chem. Soc. Rev. 35 (2006) 790–798.
[4] D. Lee, T. Cui, Biosens. Bioelectron. 25 (2010) 2259–2264.
[5] R.H. Baughman, C. Cui, A.A. Zakhidov, Z. Iqbal, J.N. Barisci, G.M. Spinks, G.G. Wallace, A. Mazzoldi, D. De Rossi, A.G. Rinzler, O. Jaschinski, S. Roth, M. Kertesz, Science 284 (1999) 1340–1344.
[6] A. Kongkanand, R.M. Dominguez, P.V. Kamat, Nano Lett. 7 (2007) 676–680.
[7] Q. Zhao, Z. Gan, Q. Zhuang, Electroanalysis 14 (2002) 1609–1613.
[8] T.R. Hesketh, J.P. Moore, J.D.H. Morris, M.V. Taylor, J. Rogers, G.A. Smith, J.C. Metcalfe, Nature 313 (1985) 481–484.
[9] H. van den Vlekkert, C. Francis, A. Grisel, N. De Rooij, Analyst 113 (1988) 1029–1033.
[10] K. Chen, G. Li, H. Lu, L. Chen, Sens. Actuators B 12 (1993) 23–27.
[11] Y. Liu, T. Cui, Sens. Actuators B 123 (2007) 148–152.
[12] W. Xue, T. Cui, Sens. Lett. 6 (2008) 675–681.
[13] C.C. Cid, J. Riu, A. Maroto, F.X. Rius, Analyst 133 (2008) 1001–1004.
[14] M. Mascini, D. Moscone, Anal. Chim. Acta 179 (1986) 439–444.
[15] E.N. Navera, K. Sode, E. Tamiya, I. Karube, Biosens. Bioelectron. 6 (1991) 675–680.
[16] P. Pandey, C. Tran-Minh, F. Lantreibecq, Appl. Biochem. Biotechnol. 31 (1991) 145–158.
[17] P.C. Pandey, S. Upadhyay, H.C. Pathak, C.M.D. Pandey, I. Tiwari, Sens. Actuators B 62 (2000) 109–116.
[18] K.M. Mitchell, Anal. Chem. 76 (2004) 1098–1106.
[19] V. Pardo-Yissar, E. Katz, J. Wasserman, I. Willner, J. Am. Chem. Soc. 125 (2002) 622–623.
[20] L.-L. Chi, L.-T. Yin, J.-C. Chou, W.-Y. Chung, T.-P. Sun, K.-P. Hsiung, S.-K. Hsiung, Sens. Actuators B 71 (2000) 68–72.
[21] Y. Liu, A.G. Erdman, T. Cui, Sens. Actuators A 136 (2007) 540–545.
[22] W. Xue, T. Cui, Sens. Actuators B 134 (2008) 981–987.
[23] W. Xue, T. Cui, J. Nano Res. 1 (2008) 1–9.
[24] D. Lee, T. Cui, J. Vac. Sci. Technol. B 27 (2009) 842–848.
[25] D. Lee, T. Cui, IEEE Sens. J. 9 (2009) 449–456.
[26] D.S. Bag, R. Dubey, N. Zhang, J. Xie, V.K. Varadan, D. Lal, G.N. Mathur, Smart Mater. Struct. 13 (2004) 1263.
[27] G. Gauglitz, T. Vo-Dinh, Handbook of Spectroscopy, Wiley, Weinheim, 2002.